JOURNAL OF CATALYSIS 130, 9–20 (1991)

The Influence of Platinum Crystallite Size on H_2 and CO Heats of Adsorption and CO Hydrogenation

B. SEN AND M. ALBERT VANNICE[1]

Department of Chemical Engineering, The Pennsylvania State University, University Park, Pennsylvania 16802

Received July 17, 1990; revised January 29, 1991

Integral heats of adsorption for H_2 and CO at 300 K were determined on SiO_2-supported Pt crystallites over a range of 1.3 to 22.3 nm and compared to those on Pt powder. No significant trend with crystallite size was observed. For H_2, the average value of 13.5 ± 2.9 kcal/mol for saturation coverage was the same as that on Pt powder, while the average value of 17 ± 5 kcal/mol for irreversible hydrogen chemisorption on the small particles was slightly lower than that on Pt powder (19.8 ± 0.8 kcal/mol). The average Q_{ad} value of 29.4 ± 3.8 kcal/mol for CO on the dispersed Pt crystallite was slightly higher than that of 27.0 ± 1.0 kcal/mol for the Pt powder, and although somewhat higher values occurred for the smallest Pt particles, the distinct increase in Q_{ad} values previously found for Pd crystallites smaller than 3 nm was not observed with Pt. No trend in the variation of the turnover frequency (TOF) for methanation with crystallite size was observed under our reaction conditions; thus this reaction is structure insensitive. However, low Pt loadings gave catalysts with lower TOFs and higher activation energies and replicated the variations in TOF reported in UHV studies of Pt. The reasons for this are not known, but the possibilities exist that either two reaction pathways may exist or the active sites on the Pt are significantly modified.

INTRODUCTION

The initial definition of a structure-sensitive reaction invoked its dependence on crystallite size (*1, 2*). Initial studies of the methanation reaction on Pt showed that the turnover frequency (TOF) was essentially unaltered as Pt crystallite size varied from 1.2 to 160 nm on an η-Al_2O_3 support, and a similar invariancy in the TOF for CH_4 appeared to exist for Pt dispersed on SiO_2 (*3, 4*); however, the TOF value on the SiO_2-supported Pt crystallites was 10-fold lower than that on the Pt/Al_2O_3 catalysts and was near that on ultrahigh purity (UHP) Pt powder (*4, 5*). Regardless, there still seemed to be some uncertainty whether methanation was a structure-sensitive reaction over Pt (*6*).

In addition to this consideration, heat of adsorption measurements for H_2 and CO on Pd showed similar increases in integral Q_{ad} values as the Pd crystallite size decreased below 3 nm (*7, 8*). Such a trend was not observed for these values on Pt, but a variety of support materials was used to obtain these latter results (*9, 10*). To remove the possibility of any support effects on either Q_{ad} or TOF values, the use of an inert support is required, and a wide range of crystallite size is desirable to clearly establish the dependence, if any, of these thermodynamic and kinetic parameters on Pt particle size. In this study, a variety of preparation techniques with an inert SiO_2 support was used to provide average Pt crystallite sizes between 1.3 and 22 nm, and both Q_{ad} and TOF values on these crystallites were compared to those measured on unsupported, UHP, 1200-nm Pt powder particles. An investigation of the former property as a function of Pt crystallite size has not been reported.

EXPERIMENTAL

SiO_2 (Davison Grade 57, 220 $m^2\ g^{-1}$) was used as the support material in this study. One catalyst was also prepared from η-

[1] To whom correspondence should be addressed.

0021-9517/91 $3.00

TABLE 1

Preparative Methods for Platinum Catalysts

Catalyst	Precursor	Method of preparation	Ref.
0.6% Pt/SiO_2	$(NH_3)_2Pt(NO_2)_2$	Incipient wetness	(*11*)
0.7% Pt/SiO_2	$Pt(NH_3)_4Cl_2$	Ion-exchange	(*12*)
2.7% Pt/SiO_2	$Pt(NH_3)_4Cl_2$	Ion-exchange	(*12*)
4.4% Pt/SiO_2	$H_2PtCl_6 \cdot 6H_2O$	Incipient wetness	(*11*)
5.0% Pt/SiO_2	$H_2PtCl_6 \cdot 6H_2O$	Incipient wetness	(*11*)
1.2% Pt/η-Al_2O_3	$H_2PtCl_6 \cdot 6H_2O$	Incipient wetness	(*11*)
1.7% Pt/SiO_2	Platinum tris(ethylene)	Low-temp. condensation	(*13*)
1.8% Pt/SiO_2	Platinum tris(ethylene)	Low-temp. condensation	(*13*)
2.2% Pt/SiO_2	Platinum tris(ethylene)	Low-temp. condensation	(*13*)

Al_2O_3 (Exxon, 245 $m^2 g^{-1}$). Prior to the preparation of the catalysts, the supports were calcined in air at 773 K for 1–4 h to remove any carbonaceous impurities. The method of preparation, metal loadings, and the catalyst precursors are listed in Table 1. A detailed description of the incipient wetness technique can be found in Ref. (*11*) while the method developed by Benesi *et al.* was used for the ion-exchanged catalysts (*12*). All the catalysts prepared from inorganic precursors were dried overnight at 393 K in air and stored in a desiccator until further use. The final platinum weight loadings were determined by neutron activation analysis using a physical mixture of $Pt(NH_3)_4Cl_2$ and the appropriate support as the standard. The unsupported UHP Pt powder was obtained from Johnson Matthey (Puratronic grade, 99.999%). Three catalyst samples prepared from a Pt tris(ethylene) complex were obtained from G. Ozin, University of Toronto (*13*). Pt crystallite size was altered further by various calcination treatments in flowing oxygen, as noted in Table 2.

The experimental systems used for measuring gas uptakes provided vacuums near 10^{-7} Torr and have been described in detail previously (*7–10*). All catalysts prepared from inorganic precursors were reduced in 20% H_2/80% He or 20% H_2/80% Ar (total flow 40–50 cm^3 min^{-1}) at 723 K for 1 h then evacuated at 698 K for 1 h before cooling *in vacuo* to 300 K, where all chemisorption measurements were made. After the initial adsorption, the samples were evacuated for 1 h and a second isotherm was obtained so that both irreversible and reversible H_2 and CO adsorption could be determined (*9–11*). For the catalysts prepared from the organic precursor, the same procedure was followed except that a reduction temperature of only 573 K was used because of the instability of Pt tris(ethylene) (*13*).

Isothermal energy changes during adsorption were measured at 300.0 K using a modified Perkin–Elmer DSC-2C differential scanning calorimeter (DSC), and a detailed description of both the calorimetric system and the method adopted for calculating energy changes after making appropriate baseline corrections has been given previously (*14*). In the DSC, the same pretreatment sequence was used except that a 1-h purge in Ar was substituted for the 1-h evacuation. All energy changes were measured at a H_2 or CO partial pressure of 10 kPa.

The kinetic data were obtained in a differential plug flow reactor using 0.1–0.5 g of catalyst and a hydrogen bracketing technique, all of which have been described previously (*3, 4, 15*). All kinetic measurements were made at 0.1 MPa (1 atm) with a H_2/CO ratio of 3 after a standard pretreatment involving a 1-h reduction at 723 K in flowing hydrogen prior to cooling to reaction temperatures.

RESULTS

The saturation (total) hydrogen uptakes and the irreversible hydrogen adsorption at

TABLE 2

Hydrogen Uptakes and Heats of Adsorption on Pt at 300 K

Catalyst	$T_{redn.}$ (K)	H_2 Uptake (μmol/g cat)		$H/Pt_{(total)}$	Pt Crystallite size[b] (nm)	Average Energy Change (mcal/g cat)		Q_{ad} (kcal/mol H_2)	
		Total[a]	Irr.[a]			Total	Irr.	Total	Irr.
1.2% Pt/η-Al_2O_3	723	37.4	25.1	1.2	1.1	540.9[a]	386.9[a]	14.5 ± 0.4	15.4 ± 0.5
0.7% Pt/SiO_2 I	723	15.2	4.7	0.85	1.3	199.7[c]	119.7[c]	13.1 ± 1.1	25.5 ± 6.2
II	723	14.1	5.5	0.79	1.4	151.6[c]	84.7[c]	10.8 ± 1.0	15.4 ± 3.3
III[d]	723	7.6	2.8	0.42	2.7	59.2[c]	22.6[c]	7.8 ± 1.3	8.1 ± 3.6
0.6% Pt/SiO_2 I[d]	723	6.2	2.9	0.40	2.8	65.6[c]	36.8[c]	10.6 ± 1.5	12.7 ± 2.9
II[e]	723	4.3	1.7	0.28	4.0	48.8[c]	21.9[c]	11.3 ± 0.4	12.9 ± 1.1
2.7% Pt/SiO_2[f]	723	12.0	6.2	0.17	6.5	171.1[c]	100.8[c]	14.6 ± 0.4	16.3 ± 0.7
4.4% Pt/SiO_2	723	21.5	9.6	0.19	5.5	357.0[a]	209.3[a]	16.6 ± 1.6	21.8 ± 3.8
5.0% Pt/SiO_2 I	723	36.9	20.2	0.29	3.9	547.7[a]	349.3[a]	14.8 ± 0.6	17.3 ± 0.8
II[g]	723	6.5	2.8	0.06	22.3	67.5[a]	30.1[a]	10.4 ± 0.3	10.8 ± 0.2
1.7% Pt/SiO_2 I	573	26.6	11.0	0.61	1.9	441.3[a]	262.8[a]	16.6 ± 0.2	23.9 ± 0.5
II[h]	573	31.6	20.7	0.73	1.6	509.4[a]	359.9[a]	16.1 ± 0.3	17.2 ± 0.5
1.8% Pt/SiO_2	573	26.0	12.8	0.56	2.0	394.8[a]	221.9[a]	15.2 ± 1.1	17.3 ± 1.7
2.2% Pt/SiO_2	573	32.4	19.7	0.70	2.0	551.7[a]	382.4[a]	17.0 ± 0.2	19.4 ± 0.5
Pt powder I	773	1.9	0.9	—	1600	25.9[c]	17.8[c]	13.6 ± 0.4	19.8 ± 0.8

[a] Average of two runs.
[b] Estimated from total H_2 uptake.
[c] Average of three runs.
[d] Calcined in 20% O_2 at 623 K for 1 h.
[e] Calcined in 20% O_2 at 623 K for $\frac{1}{2}$ h.
[f] Calcined in 36% O_2 at 773 K for 12 h.
[g] Calcined in 20% O_2 at 673 K for 21 h.
[h] Calcined in 20% O_2 at 573 K for 1 h.

300 K are listed in columns 3 and 4, respectively, of Table 2. The corresponding energy changes for each adsorption process are listed in columns 7 and 8, and these represent averge values obtained from either two or three runs, as noted. Pt dispersions (fractions exposed) and average crystallite sizes are calculated on the basis of the total hydrogen uptake and are listed in columns 5 and 6. The average crystallite sizes were calculated assuming equal areas of the (100), (110), and (111) crystal planes (*4*). The heats of adsorption for both the total H_2 uptake and the irreversible hydrogen adsorption, along with their standard deviations, are listed in columns 9 and 10. The Q_{ad} values for irreversible adsorption have, in general, a larger standard deviation because they are not directly measured quantities and uncertainties associated with both the total and reversible uptake measurements are incorporated.

The CO uptakes are listed in Table 3 in similar fashion, but the average particle sizes are those based on total hydrogen uptakes to remove any uncertainty about the adsorption stoichiometry of CO on Pt. The heats of adsorption of CO on supported Pt and Pt powder are listed in the last column along with the standard deviations.

Table 4 contains hydrogen and CO uptakes on the catalyst samples after the kinetic studies were completed, and both the final Pt crystallite sizes and the CH_4 TOF values were determined from the total H_2 uptake on these used samples. Activities, TOFs, and apparent activation energies for the methanation reaction are also given in Table 4. The low activity of the 0.6% Pt/SiO_2 and 0.7% Pt/SiO_2 samples necessitated

TABLE 3

CO Uptakes and Heats of Adsorption on Pt at 300 K

Catalyst	$T_{redn.}$ (K)	CO Uptake[a] (μmol/g cat)	$CO/Pt_{(total)}$	d (nm)	Average energy change[a] (mcal/g cat)	Q_{ad} (kcal/mol)
1.2% Pt/η-Al_2O_3	723	44.2	0.72	1.1	939.5	21.3 ± 1.2
0.7% Pt/SiO_2 I	723	16.1	0.45	1.3	515.0	32.0 ± 0.7
II	723	17.6	0.49	1.4	527.9	30.0 ± 1.4
III[b]	723	9.7	0.27	2.7	250.3	25.8 ± 2.2
0.6% Pt/SiO_2 I[b]	723	5.5	0.18	2.8	169.9	30.9 ± 1.5
II[c]	723	5.8	0.19	4.0	166.6	28.7 ± 1.4
2.7% Pt/SiO_2[d]	723	11.1	0.08	6.5	337.9	30.4 ± 0.7
4.4% Pt/SiO_2	723	25.4	0.11	5.5	976.8	38.5 ± 0.8
5.0% Pt/SiO_2 I	723	56.1	0.22	3.9	1486.6	26.5 ± 0.8
II[e]	723	11.2	0.04	22.3	250.7	22.4 ± 1.9
1.7% Pt/SiO_2 I	573	46.0[f]	0.53	1.9	1336.7[f]	29.1
II[g]	573	44.6[f]	0.51	1.6	1398.6[f]	31.4
1.8% Pt/SiO_2	573	48.3[f]	0.52	2.0	1285.5[f]	26.6
2.2% Pt/SiO_2	573	50.2[f]	0.45	2.0	1514.0[f]	30.2
Pt powder I	773	2.6		1600	72.4	27.8 ± 0.3
II	773	2.4		1600	62.9	26.2 ± 1.4

[a] Average of two runs.
[b] Calcined in 20% O_2 at 623 K for 1 h.
[c] Calcined in 20% O_2 at 673 K for ½ h.
[d] Calcined in 36% O_2 at 773 K for 12 h.
[e] Calcined in 20% O_2 at 673 K for 2 h.
[f] Only one measurement.
[g] Calcined in 20% O_2 at 573 K for 1 h.

conducting the kinetic runs at higher temperatures (553–643 K) and extrapolating to 548 K for comparison. Regardless, the higher activation energies observed in this region are not completely responsible for the low TOF values compared to the higher loading catalysts, and a comparison at a temperature common for all catalysts (588 K) still gave lower TOFs although the spread in values ($0.9–5.3 \times 10^{-4}$ s^{-1}) was smaller.

DISCUSSION

Hydrogen Adsorption

Numerous values for heats of adsorption of hydrogen on Pt have been reported in the literature (*16–32*), and they are summarized in Table 5. Although most represent initial Q_{ad} values, in some cases where enough data were available integral Q_{ad}'s have been estimated, and they are also listed because they provide the best comparisons to our isothermal, integral heats of adsorption which were measured calorimetrically. In particular, some recent studies have provided differential heats on SiO_2-supported Pt from which integral Q_{ad} values can be calculated (*29–32*). Even on one single crystal—Pt(111)—initial Q_{ad} values have varied from 10 to 20 kcal mol^{-1}, and a wide range from 8 to 30 kcal mol^{-1} exists for the various adsorbed states of hydrogen on a variety of Pt surfaces. The estimated integral values also cover a wide range of 9 to 25 kcal mol^{-1}, and no discernible relationship clearly emerges to indicate a correlation between surface structure and the heat of adsorption. Fewer studies have been conducted on supported Pt catalysts (*10, 28–32*). Lantz and Gonzalez calorimetrically measured heats of adsorption for hydrogen on 1.4 to 1.8 nm Pt crystallites on SiO_2 and they concluded that the integral Q_{ad} values for H_2 were near

TABLE 4

Adsorption on Used Pt Catalysts and Kinetic Behavior for Methanation

Catalyst	Sample	d^a (nm)	Uptake (μmol/g cat)			Activity[b] μmol $CH_4 \times 10^4$ s g cat	$N_{CH_4}{}^{a,b}$ ($s^{-1} \times 10^4$)	E_{act} (kcal/mol)
			H_2 (Tot.)	H_2 (Irr.)	CO			
0.7% Pt/SiO_2	I	1.1	20.5	11.2	29.3	4.5	0.1	39
	II	2.0	10.4	4.4	14.5	5.6	0.3	29
	III	4.8	4.2	—	6.3	2.3	0.3	26
	IV	6.8	3.0	—	—	0.8	0.1	29
0.6% Pt/SiO_2		11.6	1.5	—	2.2	0.9	0.3	30
1.0% Pt/SiO_2		1.6	17.8	6.8	—	51	1.4	20
2.7% Pt/SiO_2	I	4.9	15.9	9.4	15.8	54	1.7	18
	II	1.6	49.3	27.0	68.8	148	1.5	19
4.4% Pt/SiO_2	I	4.3	29.6	13.0	38.6	47	0.8	21
	II	8.0	16.0	8.4	30.0	38	1.2	21

[a] Based on total H_2 uptake on used sample.
[b] At 548 K, $H_2/CO = 3$ and $P_T = 1$ atm.

16 kcal/mol and essentially independent of Pt crystallite size; however, the initial Q_{ad} values decreased slightly as particle size decreased (*29*). A somewhat higher Q_{ad} value of 24.5 kcal/mol is obtained from the results of Aukett for 2-nm Pt crystallites (*31*), whereas the value of 16.5 kcal/mol from the data of Goddard *et al.* (*32*) is in excellent agreement with that of Lantz and Gonzalez (*29*) and our earlier values near 16.6 kcal/mol for irreversible adsorption (*10*). Takasu *et al.* found the activation energy for H_2 desorption increased from 8 kcal mol^{-1} on 1.6-nm Pt particles to 12 kcal mol^{-1} on 4.3-nm Pt particles dispersed on SiO_2 (*28*); however, effects of pore diffusion and readsorption (*33, 34*), which were not considered, make these values suspect. Mills *et al.* have reported H_2 heats of adsorption near 30 kcal mol^{-1} on a 6.2% Pt/SiO_2 catalyst (*30*); however, this value is erroneously high because they were using N_2 as the carrier gas in their DSC (*10*). Sermon and co-workers have also studied the energetics of hydrogen chemisorption on supported Pt catalysts, and they did not observe any noticeable change in the binding energy of H_2 on crystallite sizes ranging from 1.1 to 16.6 nm on SiO_2 although the relative populations of the three desorption states were found to change with dispersion (*35, 36*).

In the present study, integral heats of adsorption of hydrogen were measured for a family of silica-supported Pt catalysts providing a crystallite size range from 1.3 to 22.3 nm. The DSC was operated under optimum conditions described earlier (*10*). The average heat of adsorption for saturation hydrogen coverage was 13.5 ± 2.9 kcal mol^{-1}, which is in excellent agreement with both the Q_{ad} value of 13.6 kcal mol^{-1} obtained for Pt powder and the average Q_{ad} of 13.5 ± 2 kcal mol^{-1} determined for Pt on a variety of supports (*10*). It is also very consistent with the estimated integral Q_{ad} values in Table 5. For irreversible hydrogen adsorption, the average Q_{ad} is 17 ± 5 kcal mol^{-1}. The variations of both these Q_{ad} values as a function of Pt crystallite size are shown in Fig. 1. Several conclusions can be drawn. First, although there is some variation among the data for total coverage in Fig. 1a, with the exception of one sample all Q_{ad} values fall between 10.4 and 17.0 kcal/mol, and there is clearly no trend as the Pt crystallite size decreases and approaches 1 nm. The results for irreversible hydrogen adsorption in Fig. 1b are indirectly obtained from the differ-

TABLE 5

Initial and Integral Heats of Adsorption of H_2 on Pt

Surface	State	Initial $Q_{(ad)}$ (kcal/mol)	Integral $Q_{(ad)}$[a] (kcal/mol)	Method[b]	Ref.
(111)		16	12	ISO	(*16*)
(111)		9.5	9	ΔΦ	(*17*)
(111)		17.5	16	TPD	(*18*)
(111)		17.5		TPD	(*19*)
(111)		17		FEM	(*20*)
(111)	α, β	15–32		TPD	(*21*)
(110)	β_1, β_2	9.8–13.1	9–12	TPD	(*18*)
(110)		26		FEM	(*22*)
(110)	α, β	14–22		FEM	(*20*)
(100)	β_1–β_5	9.1–27.5		TPD	(*18*)
(100)	α, β	16–24		FEM	(*20*)
(100)		15–16		TPD	(*23*)
(210)		20.2	20	TPD	(*18*)
(210)	α, β	16–26			(*20*)
(211)	α, β	16.0–21.0	15	TPD	(*18*)
9(111) × (111)		20.0			(*24*)
Film	γ, β_1, β_2	8–21		TPD	(*25*)
Filament		24.7	20	CAL	(*26*)
Filament	α, β	16–25		FEM	(*20*)
Film		21.3	17	CAL	(*27*)
Pt/SiO_2		8.1–11.9		TPD	(*28*)
Pt/SiO_2			16.6 (ave)	CAL	(*10*)
Pt/SiO_2			16	CAL	(*29*)
Pt/SiO_2			30	CAL	(*30*)
Pt/SiO_2		26.3	24.5	CAL	(*31*)
Pt/SiO_2		20	16.5	CAL	(*32*)

[a] Estimated at monolayer coverage.

[b] Isosteres—ISO; work function change—ΔΦ; temperature-programmed desorption—TPD; field ion microscopy—FEM; calorimetry—CAL.

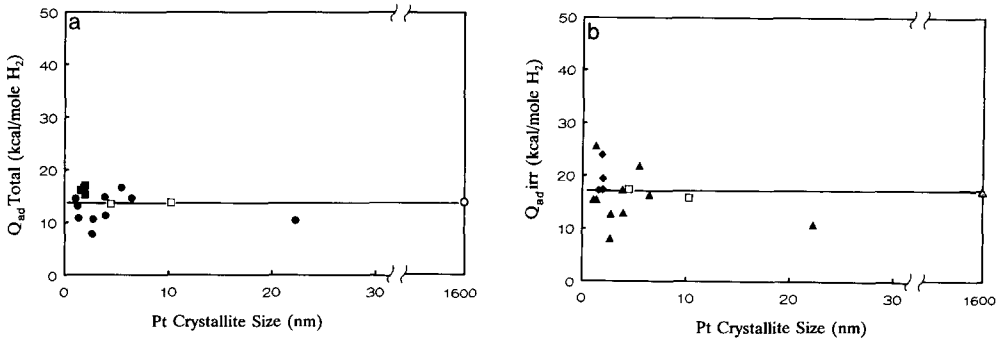

FIG. 1. Integral heats of adsorption for (a) saturation coverage and (b) irreversible hydrogen adsorption on silica-supported Pt as a function of crystallite size (P_{H2} = 10 kPa, T = 300 K): ●, ▲, Pt/SiO_2 prepared from inorganic precursor; ■, ◆, Pt/SiO_2 prepared from organometallic precursor; ○, △, Pt powder; □ from Ref. (*10*). The line denotes the average value.

ence between total and reversible adsorption and they exhibit noticeably more scatter; regardless, there is again no dependence on crystallite size within the uncertainty of the data. Second, these results are in excellent agreement with our previous values for Pt/SiO_2 (*10*) and those reported for Pt/SiO_2 by Lantz and Gonzalez (*29*) and Dumesic and co-workers (*32*). Third, a sintering step in oxygen seems to increase the probability of low Q_{ad} values because the lowest Q_{ad} values were obtained with calcined samples. The initial Q_{ad} values for hydrogen in Table 5 are similar on different planes; thus the reason for the low values is not clear at this time. Finally, the absence of an increase in Q_{ad} on very small Pt particles indicates different behavior compared to Pd, which exhibited an increase in Q_{ad} values on Pd crystallites smaller than 3 nm (*7*). Both the independence of Q_{ad} values from Pt crystallite size and the average Q_{ad} shown in Fig. 1(a), reproduce the behavior shown for Pt in Fig. 2 of Ref. (10), which utilized Al_2O_3, SiO_2–Al_2O_3, and TiO_2 as well as SiO_2 as supports. This implies little, if any, support effect on integral hydrogen adsorption properties on Pt when typical supports are employed.

Carbon Monoxide Adsorption

To allow a thorough comparison and to illustrate the rather wide range of values, even on the same crystal plane, initial heats of adsorption of CO on Pt single crystals, foils, films, and other surfaces have been gathered in Table 6 (*19, 37–57*), and integral heats have again been calculated whenever data regarding the variation of Q_{ad} with coverage were given. All the estimated integral heats obtained under UHV conditions fall between 25 and 35 kcal mol^{-1}, and they can be compared with the average Q_{ad} value of 29.4 ± 3.8 found here for the 1.3 to 22 nm Pt crystallites dispersed on SiO_2. On the (111) plane the integral Q_{ad} is 26 kcal mol^{-1}, which is in very good agreement with the average value near 27 kcal mol^{-1} that was obtained for the Pt powder on which (111) planes should predominate. With the exception of the sintered 5% Pt/SiO_2 sample which gave a low Q_{ad} of 22.4 kcal mol^{-1} and the 4.4% Pt/SiO_2 sample which produced an unusually high value of 38.5 kcal mol^{-1}, the variation among the Q_{ad} values was not great. These Q_{ad} values were again in excellent agreement with previous ones we reported for Pt/SiO_2 (*9*), the values fall between those reported recently by Aukett (*31*) and Goddard *et al.* (*32*), which are shown in Table 6, and they indicate that statistically there is little, if any, increase in Q_{ad} for CO on Pt crystallites smaller than 5 nm, as shown in Fig. 2. The heat of adsorption of CO on the 1.2% Pt/Al_2O_3 sample (1.1-nm crystallites) was 21.3 kcal mol^{-1}, which was noticeably lower than the values obtained on silica-supported Pt but in good agreement with the values near 24 kcal mol^{-1} reported earlier for well-dispersed Pt on Al_2O_3 (*9*) and the Q_{ad} of 18 kcal mol^{-1} for 1-nm Pt particles on Al_2O_3 reported by Herz and McCready (*56*).

As Table 6 shows, higher energy binding states for CO routinely exist on a variety of the more open Pt crystal planes; thus the distribution of these surfaces could easily produce some of the differences in the observed Q_{ad} values that are apparent in Fig. 2. Doering *et al.* studied CO chemisorption on particulate Pt films on mica and observed two desorption peaks: one at 393 K attributed to smooth Pt surfaces and another at 448 K attributed to edges and steps (*58*). The latter peak was a larger fraction of the total CO desorption flux from small (1.5 to 4.0 nm) particles, but it was a minor contributor for a continuous film. Zhu and Schmidt have also observed stronger binding states for CO on small Pt particles compared to larger particles supported on SiO_2 (*59*). Therefore, a small increase in the heat of adsorption of CO on Pt crystallites smaller than 5 nm would be consistent with these two studies as well as other UHV studies in Table 6, and the simplest explanation is that small Pt particles possess rougher surfaces and larger concentrations of edge and step sites,

TABLE 6

Initial and Integral Heats of Adsorption of CO on Pt

Surface	State	Initial $Q_{(ad)}$ (kcal/mol)	Integral $Q_{(ad)}$[a] (kcal/mol)	Method[b]	Ref.
(111)		24–27		TPD	(37)
(111)		17.5		TPD	(19)
(111)	β_1, β_2	22.3–30.2	26	TPD	(38)
(111)	Linear	26.7–29.6		TPD	(39)
	Bridged	25–27			
(111)	β_1, β_2	22.7–29.6	26	TPD	(40)
(111)		28.0		TPD	(41)
(111)		34.5		TPD	(42)
(111)		30–34		$\Delta\Phi$	(43)
100 (1 × 1)		37.5		TPD	(44)
100 (5 × 20)		27.5		TPD	(44)
(100)	β_1, β_4	23.6–31.9		TPD	(40)
(100) (5 × 20)		28.1–33.1		TPD	(45)
(110)	β_1. β_2	19.8–26.0	25	TPD	(40)
(110)		38.1	35	ISO	(46)
(110)		35.3		TPD	(47)
(110)	β_1, α_2, α_3	25.1–31.4		TPD	(48)
(110)	α, β	25.0–30.7		TPD	(49)
6(111) × (111)	α_1, α_2	24–33		TPD	(37)
(200)	β_L, β_H	27.1–36.2	35	TPD	(40)
(211)	β_L, β_H	27.1–35.2	32	TPD	(40)
(410)		22–32		TPD	(50)
(321)		23–36		TPD	(51)
(12,11,9)		36		$\Delta\Phi$	(43)
Foil	α_1, α_2	25–32		TPD	(37)
Foil	α_1, α_2	25.7–31.7		TPD	(52)
FEM Tip		32		$\Delta\Phi$	(22)
Film		44	44	CAL	(53)
Polycrystalline	α, β	25–32		TPD	(54)
Ribbon		32–37		TPD	(55)
Pt/Al_2O_3		18		TPD	(56)
Pt/SiO_2		—	27.0	CAL	(9)
Pt/SiO_2		38.2	34.6	CAL	(31)
Pt/SiO_2		28	23.4	CAL	(32)
Pt/SiO_2		29.9	20.3	CAL	(57)

[a] Estimated at monolayer coverage.
[b] For nomenclature see Table 5.

which can have higher binding energies. Regardless, such an increase is small (ca. 2 kcal/mol) and clearly less obvious than the increase of over 10 kcal/mol found for CO adsorption on Pd as crystallite size decreased below 3 nm (*8*). The reason for the difference between the two metals is not clear, but it may be due to the higher energy of the Pd valence band compared to that of Pt. Theoretical studies by Anderson and Awad have shown that this enhancement in surface back-donation to the CO π^* orbitals favors adsorption on higher coordination sites on Pd (by 10–14 kcal/mol), whereas adsorption on one- and twofold sites is favored on Pt(111) and Pt(100) and the energy difference between these two sites is smaller, being about 8 kcal/mol on Pd(111) and 0.7 kcal/mol on the Pt(100) surface (*60*). Thus any variation would be anticipated to

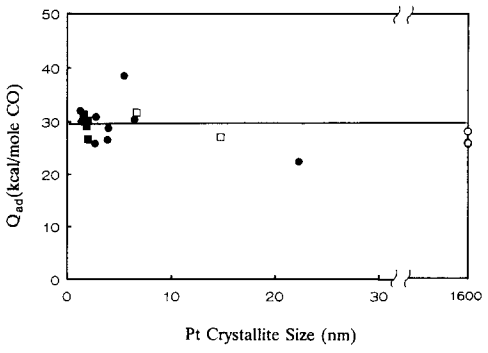

FIG. 2. Integral heats of adsorption of CO on silica-supported Pt as a function of crystallite size (P_{CO} = 10 kPa, T = 300 K): ● prepared from inorganic precursor; ■ prepared from organometallic precursor; ○ Pt powder; □ from Ref. (*9*). The line denotes the average value.

be smaller based on these calculations. Despite the variations, a strong dependence of integral heats of adsorption of CO versus Pt crystallite size does not exist; consequently, the significant decrease in Q_{ad} as the CO/Pt ratio increased that was found by Vannice and co-workers (*9*) must be attributed to a support effect, rather than a crystallite size effect. This may account for the lower Q_{ad} values previously obtained for highly dispersed Pt/Al_2O_3 samples (*9*, *56*) and for the Pt/Al_2O_3 catalyst in Table 3. The calculations of Anderson and Awad indicate that a decrease in the valence state ionization potential for Pt would produce a corresponding decrease in the CO binding energy (*60*), and a lower energy binding state for CO on very small Al_2O_3-supported Pt particles has been reported by Herz and McCready (*56*).

CO Hydrogenation

The kinetic properties of these silica-supported Pt catalysts for methanation are listed in Table 4. The TOFs and activation energies of the higher Pt loading (1.0% and above) catalysts are very consistent with previous results, as the average TOF for these five samples is 1.3×10^{-4} s^{-1} compared to values between 1.4×10^{-4} and 1.9×10^{-4} s^{-1} reported previously for Pt/SiO_2 catalysts (*4*) and a value of 1.1×10^{-4} s^{-1} for ultrahigh purity Pt powder obtained by Vannice and Sudhakar (*5*). An examination of these and previous TOF values versus Pt crystallite size clearly shows that the TOF is essentially invariant on particles ranging from 1.6 to 1600 nm, as illustrated in Fig. 3. This lack of dependence of TOF on Pt crystallite size is consistent with previously reported results for Al_2O_3-supported Pt (*4*) and Pd (*61*), and it, along with a recent study of $Pd–Cu/SiO_2$ catalysts (*62*), provides additional confirmation that methanation is not a structure-sensitive reaction on these two noble metals.

The five samples from the two catalysts with low Pt loadings (0.6 and 0.7%) provided TOFs that varied little ($0.2 \pm 0.1 \times 10^{-4}$ s^{-1}) and E_{act} values that fell between 26 to 39 kcal/mol. These TOFs are noticeably lower and the activation energies are distinctly higher than those obtained with other Pt/SiO_2 catalysts, and they do not appear to be dependent upon the Pt precursor or the use of a calcination step or the Pt dispersion. These latter E_{act} values are very similar to those of 25 kcal/mol reported by Dwyer *et al.* for a clean Pt black sample (*63*) and 30 kcal/mol reported by Demmin *et al.* for a Pt foil (*64*), and the lower TOF values in our study tend to be closer to the value near 6

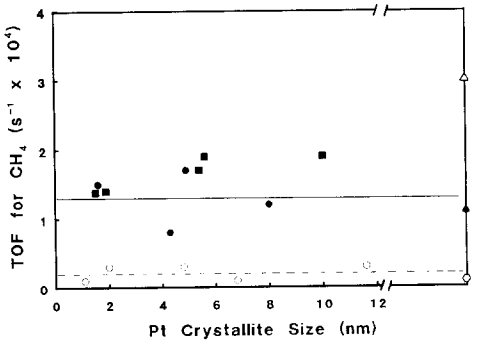

FIG. 3. Turnover frequencies for CH_4 formation on Pt versus crystallite size (T = 548 K, H_2/CO = 3, P_T = 1 atm); ● Pt/SiO_2, this study, ■ Pt/SiO_2, from Ref. (*4*); ○ Pt powder, from Ref. (*5*), ⬡ Pt black, from Ref. (*63*); △ Pt foil, from Ref. (*64*). Solid line, average value from higher loading Pt/SiO_2 catalysts; dotted line, average value from 0.6 and 0.7% Pt/SiO_2.

$\times 10^{-6}$ s^{-1} obtained by the former authors (*63*) than the value of 3×10^{-4} s^{-1} reported by the latter group (*64*). Rather than omit these results, we chose to include them even though we do not have a good explanation for this order-of-magnitude variation in TOF which appears to occur on Pt surfaces prepared under UHV conditions as well as on SiO_2-supported Pt. It is worth noting that all the high activation energies were obtained in a higher-temperature region i.e., 525–715 K in Ref. (*63*), 588–1000 K in Ref. (*64*), and upper temperatures above 640 K with the 0.6% Pt/SiO_2 and 0.7% Pt/SiO_2 catalysts in Table 4. For a well-dispersed Pt/SiC catalyst containing some residual free carbon, TOF and E_{act} values very similar to the higher loading Pt/SiO_2 catalysts were obtained at 548 K after reduction at either 443 or 773 K (0.9-1.1 $\times 10^{-4}$ s^{-1} and 16-22 kcal/mol, respectively); however, after the latter reduction step the Arrhenius plot showed a distinct increase from 16 kcal/mol in the temperature region below 613 K to 27 kcal/mol in the region between 613 and 663 K (*65*). Calcination of this support to facilitate carbon removal prior to impregnation gave higher TOFs closer to those found with Pt/Al_2O_3 catalysts and eliminated this shift to a higher activation energy (*65*). Demmin *et al.* have mentioned that a high-temperature O_2 exposure gave TOF values an order of magnitude lower than their steady-state rates (*64*). Consequently, we suggest the possibility that carbon (or perhaps strongly bound oxygen) on the Pt may be a factor in this behavior.

The methanation reaction is near first order in H_2 and zero order in CO; thus it is nearly independent of the CO heat of adsorption and the apparent activation energy is essentially the difference between the activation energy of the rate-determining step and the H_2 heat of adsorption (*4*). Consequently, it is possible that a lower Q_{ad} value for H_2 could increase the observed E_{act} value, but the deviations in Table 2 from the average value of 13.5 kcal/mol do not appear large enough to explain the higher apparent activation energies for the low loading samples. The variation in the E_{act} values and the transition to a higher activation energy at higher temperatures raise the possibilities that either a different reaction mechanism may exist or the active sites on the Pt are significantly modified. Should such an alternative reaction sequence exist, it appears to occur on very small Pt crystallites as well as on bulk Pt surfaces. Further studies are required to explain this variation in TOF and to determine if more than one reaction sequence exists on Pt, particularly in the higher temperature regime. Regardless, in the reaction regime utilized here structure insensitivity is clearly indicated by the lack of dependence of TOF on crystallite size for Pt/SiO_2 catalysts with weight loadings of 1% or above, and even after considering the small (ca. 10-fold or less) variation in TOF among *all* the unsupported and SiO_2-supported Pt catalysts in Table 4, one can still classify methanation on Pt as structure insensitive according to the original definition of this term (*1, 2, 66*).

SUMMARY

The integral heats of adsorption for either saturation coverage or irreversible hydrogen adsorption on SiO_2-supported Pt showed no dependence on crystallite size between 1.3 and 22.3 nm, and the average Q_{ad} of 13.5 kcal mol^{-1} for total coverage was the same as that on Pt powder and Pt dispersed on η-Al_2O_3, SiO_2–Al_2O_3, and TiO_2 (reduced at 473 K). A sintering step in O_2 appeared to induce more scatter in the results by producing the lowest Q_{ad} values measured. All CO chemisorption was irreversible and, although Q_{ad} did not vary extensively, there was a small increase from 27 on Pt powder to 30 kcal mol^{-1} as Pt crystallite size approached 1 nm. This is most likely due to the distribution of crystal planes as Q_{ad} values are higher on the more open single-crystal surfaces; however, the concentrations of edge, corner, step, and kink sites may also play a role. The absence of a strong increase in the heat of adsorption

of either H_2 or CO as Pt crystallite sizes drop below 3 nm is in contrast to the behavior exhibited by Pd (*7, 8*). The precise reason for this is not known, but it is currently attributed to the higher energy level of the Pd valence band compared to Pt and the smaller variation in the CO binding energy that results for Pt (*60*).

Although an order of magnitude variation was found in TOFs for methanation, the spread originated from two catalysts with low Pt loadings pretreated in different ways and, in fact, a similar divergence in TOF values has been reported for clean Pt black and Pt foil samples (*63, 64*). However, within either group of catalysts there was no dependence of TOF on Pt crystallite size; consequently, the methanation reaction can be classified as structure insensitive. Although the higher apparent activation energies associated with the less active Pt surfaces may be partially caused by lower Q_{ad} values for H_2, this variation is not sufficient to produce the high values. It is more likely that the high E_{act} values may represent a change in the reaction mechanism or a modification of the active sites on the Pt surface. The low TOF values that are invariant not only with the size of Pt crystallites on SiO_2 but also with changes in the heat of adsorption of CO clearly show that the higher TOF values obtained with Al_2O_3, SiO_2–Al_2O_3, and TiO_2 must be due to a support effect in some manner. An earlier study found that when these other supports were used, CO heats of adsorption decreased and a concomitant increase in the TOF occurred (*9*); however, the present results imply that this is not a cause and effect relationship but rather two variables being altered simultaneously as a consequence of a change (or changes) at the Pt surface.

ACKNOWLEDGMENTS

We thank Professor G. Ozin for providing the Pt/SiO_2 samples prepared from Pt tris(ethylene) and Shawn Lin for conducting the experiments with the 1.0% Pt/SiO_2 catalyst. This study was supported by the U.S. Department of Energy, Division of Basic Energy Sciences, under Grant DE-FG02-84ER13276.

REFERENCES

1. Boudart, M., *in* "Advances in Catalysis" (D. D. Eley, H. Pines, and P. B. Weisz, Eds.), Vol. 20, p. 153. Academic Press, New York, 1969.
2. Boudart, M., *J. Mol. Catal.* **30,** 27 (1985).
3. Vannice, M. A., Twu, C. C., and Moon, S. H., *J. Catal.* **79,** 70 (1983).
4. Vannice, M. A., and Twu, C. C., *J. Catal.* **82,** 213 (1983).
5. Vannice, M. A., and Sudhakar, C., *J. Phys. Chem.* **88,** 2429 (1984).
6. Boudart, M., and McDonald, M. A., *J. Phys. Chem.* **88,** 2185 (1984).
7. Chou, P., and Vannice, M. A., *J. Catal.* **104,** 1 (1987).
8. Chou, P., and Vannice, M. A., *J. Catal.* **104,** 17 (1987).
9. Vannice, M. A., Hasselbring, L. C., and Sen, B., *J. Catal.* **97,** 66 (1986).
10. Sen, B., Chou, P., and Vannice, M. A., *J. Catal.* **101,** 517 (1986).
11. Palmer, M. B., and Vannice, M. A., *J. Chem. Technol. Biotech.* **30,** 205 (1980).
12. Benesi, H. A., Curtis, R. M., and Studer, H. P., *J. Catal.* **10,** 328 (1968).
13. Ozin, G., Private Communication; Prokopowitz, R., Ph.D thesis, University of Toronto, 1989.
14. Vannice, M. A., Sen, B., and Chou, P., *Rev. Sci. Instrum.* **58,** 647 (1987).
15. Vannice, M. A., Moon, S. H., and Wang, S.Y., *J. Catal.* **71,** 152 (1981).
16. Norton, P. R., Davies, J. A., and Jackman, T. E., *Surf. Sci.* **121,** 103 (1982).
17. Christmann, K., Ertl, G., and Pignet, T., *Surf. Sci.* **54,** 365 (1976).
18. McCabe, R. W. and Schmidt, L. D., *in* "Proceedings, 7th International Vacuum Congress, Vienna, 1977," p. 1201.
19. Lu, K. E., and Rye, R. R., *Surf. Sci.* **45,** 677 (1974).
20. Nieuwenhuys, B. E., *Surf. Sci.* **59,** 430 (1976).
21. Weinberg, W. H., Monroe, D. R., Lampton, V., and Merrill, R. P., *J. Vac. Sci. Technol.* **14,** 444 (1977).
22. Rootsaert, W. J. M., van Reijen, L. L., and Sachtler, W. M. H., *J. Catal.* **1,** 416 (1962).
23. Netzer, F. P., and Kneringer, G., *Surf. Sci.* **51,** 526 (1975).
24. Poelsema, B., Mechtersheimer, G., and Comsa, G., *Surf. Sci.* **111,** 519 (1981).
25. Stephan, J. J., Ponec, V., and Sachtler, W. M. H., *J. Catal.* **37,** 81 (1975).
26. Norton, P. R., and Richards, P. J., *Surf. Sci.* **44,** 129 (1974).
27. Cerny, S., Smutek, M., and Buzek, F., *J. Catal.* **38,** 245 (1975).
28. Takasu, Y., Teramoto, M., and Matsuda, Y., *J. Chem. Soc. Chem. Commun.*, 1329 (1983).

29. Lantz, J. B., and Gonzalez, R. D., *J. Catal.* **41,** 293 (1976).
30. Mills, E. R. A., Sermon, P. A., and Wuri, A. J., *in* "Proceedings, 8th International Congress on Catalysis, Berlin, 1984." Dechema, Frankfurt-am-Main, 1984.
31. Aukett, P. N., *in* "Structure and Reactivity of Surfaces" (C. Morterra *et al.*, Eds.), p. 11. Elsevier, Amsterdam, 1989.
32. Goddard, S. A., Amiridis, M. D., Rekoske, J. E., Cardona-Martinez, N., and Dumesic, J. A., *J. Catal.* **117,** 155 (1989).
33. Herz, R. K., Kiela, J. B., and Marin, S. P., *J. Catal.* **73,** 66 (1982).
34. Gorte, R. J., *J. Catal.* **75,** 164 (1982).
35. Hoyle, N. D., Newbatt, P. H., Rollins, K., Sermon, P. A., and Wurie, A. T., *J. Chem. Soc. Faraday Trans 1* **81,** 2605 (1985).
36. Vong, M. S. W., and Sermon, P. A., *J. Chem. Soc. Faraday Trans. 1* **83,** 1369 (1987).
37. Collins, D. M., and Spicer, W. E., *Surf. Sci.* **69,** 85 (1977).
38. McCabe, R. W., and Schmidt, L. D., *Surf. Sci.* **65,** 189 (1977).
39. Norton, P. R., Goodale, J. W., and Selkirk, E. B., *Surf. Sci.* **83,** 189 (1979).
40. McCabe, R. W., and Schmidt, L. D., *Surf. Sci.* **66,** 101 (1977).
41. Ertl, G., Neumann, M., and Streit, K. M., *Surf. Sci.* **64,** 393 (1977).
42. Steininger, H., Lehwald, S., and Ibach, H., *Surf. Sci.* **123,** 264 (1982).
43. Poelsema, B., Palmer, R. L., and Comsa, G., *Surf. Sci.* **123,** 152 (1982).
44. Thiel, P. A., Behm, R. J., Norton, P. R., and Ertl, G., *Surf. Sci.* **121,** L553 (1982); *J. Chem. Phys.* **78,** 7448 (1983).
45. Barteau, M. A., Ko, E. I., and Madix, R. J., *Surf. Sci.* **102,** 99 (1981).
46. Jackman, T. E., Davies, J. A., Jackson, D. P., Unertl, W. N., and Norton, P. R., *Surf. Sci.* **120,** 389 (1982).
47. Fair, J., and Madix, R. J., *J. Chem. Phys.* **73,** 3480 (1980).
48. Bonzel, H. P., and Ku, R., *J. Chem. Phys.* **58,** 4617 (1973).
49. Comrie, C. M., and Lambert, R. M., *J. Chem. Soc. Faraday Trans. 1* **72,** 1659 (1976).
50. Park, Y. O., Banholzer, W. F., and Masel, R. I., *Surf. Sci.* **155,** 341 (1985).
51. McClellan, M. R., Gland, J. L., and McFeely, F. R., *Surf. Sci.* **112,** 63 (1981).
52. Winterbottom, W. L., *Surf. Sci.* **37,** 195 (1973).
53. Brennan, D., and Hayes, F. H., *Philos. Trans. Roy. Soc. A* **258,** 347 (1965).
54. Collins, D. M., Lee, J. B., and Spicer, W. E., *Surf. Sci.* **55,** 389 (1976).
55. Shigeishi, R. A., and King, D. A., *Surf. Sci.* **58,** 379 (1976).
56. Herz, R. K., and McCready, D. F., *J. Catal.* **81,** 358 (1983).
57. Efremov, A. A., Bakhmutova, N. I., Pankratiev, Yu. D., and Kuznetsov, B. N., *React. Kinet. Catal. Lett.* **28,** 103 (1985).
58. Doering, D. L., Poppa, H., and Dickinson, J. T., *J. Vac. Sci. Technol.* **20,** 827 (1982).
59. Zhu, Y., and Schmidt, L. D., *Surf. Sci.* **129,** 107 (1983).
60. Anderson, A. B., and Awad, Md. K., *J. Am. Chem. Soc.* **107,** 7854 (1985).
61. Wang, S.-Y., Moon, S. H., and Vannice, M. A., *J. Catal.* **71,** 167 (1981).
62. Leon y Leon, C. A., and Vannice, M. A., *Appl. Catal.* **69,** 305 (1991).
63. Dwyer, D. J., Robbins, J. L., Cameron, S. D., Dudash, N., and Hardenbergh, J., *ACS Symp. Ser.* **298,** 21 (1986).
64. Demmin, R. A., Ko, C. S., and Gorte, R. J., *J. Phys. Chem.* **89,** 1151 (1985).
65. Vannice, M. A., Chao, Y-L., and Friedman, R. M., *Appl. Catal.* **20,** 91 (1986).
66. Boudart, M., *in* "Proceedings, 6th International Congress on Catalysis" (G. C. Bond, P. B. Wells, and F. C. Tompkins, Eds.), Vol. 1, p. 1. Elsevier, Amsterdam, 1976.